Studentischer Beitrag zum 45. IWASA 2015

Using background potential energy to quantify turbulent entrainment in a wind-driven stratified fluid layer

Magnus Beyer, Holger Schüttrumpf und Maarten van Reeuwijk

Abstract

It is well known that turbulent entrainment has an important influence on the ecological stability of deep lakes e.g. water reservoirs and mining lakes. Much remains to be uncovered about the physics of turbulent entrainment in these stratified fluid layers, especially the determination of the entrainment rate. The aim of this study was to determine the entrainment rate based on background potential energy (BPE) applying Direct Numerical Simulation (DNS) of a sheared fluid layer. Simulations were performed on a grid of 15m x 5m x 8m at a resolution of 768 x 256 x 640. The preliminary results indicate that the entrainment rate based on BPE is almost free of statistical variance and more reliable than commonly applied methods.

1 Introduction

Fluids of different density stratify where a dense fluid gathers beneath a lighter fluid forming two layers. This density difference can be due to e.g. temperature gradients and it occurs regularly in environment e.g. in lakes, the atmosphere or with regard to building ventilation. Shear acting on the top or bottom surface induces turbulence *leading to a mixed layer. This mixed layer is bounded by an interface that sits between the mixed layer and the quiescent layer and will deepen with time as a result of turbulence. This deepening, which involves turbulence "eating into" the quiescent layer, is called turbulent entrainment. The interface between the quiescent layer and the mixed layer suppresses the vertical transport and is therefore of great importance*.

There is a large uncertainty about the determination of the rate at which the mixed layer deepens (Fernando, 1991). This so-called entrainment rate has been measured in field experiments and laboratory experiments. However, even the laboratory experiments, which offer much more control (in terms of initial boundary conditions and parameter values) than field experiments, report differences as large as a factor 5 (Fernando, 1991). A better understanding of entrainment of stratified fluids is necessary to allow for a better insight into the physics of transport across density-stratified layers.

This report addresses stratification and entrainment using lakes as an example. Causes of mixing and causes of stratification in lakes are briefly outlined of in section 2 (a more detailed description of mixing and stratification in lakes can be found in Beyer, 2014). Section 3 presents the fundamental physical understanding of entrainment in stratified fluid layers and a description of the numerical simulations that have been investigated. Section 4 introduces and discusses an indicator based on background potential energy (BPE) that appears suitable to determine the entrainment rate. Section 5 concludes with final remarks.

2 Mixing and stratification in lakes

The vertical structure of a lake consists of an upper layer, the epilimnion, a lower layer, the hypolimnion and an interface between these layers, the thermocline. The epilimnion is well-mixed due to wind shearing the surface and heated by solar radiation. Because the heated epilimnion is well-mixed it is of almost homogeneous temperature and warmer than the hypolimnion. The hypolimnion comprises calm, colder water. In the hypolimnion, mixing is very sporadic and confined to isolated patches (Sokolofsky & Jirka, 2004). The separating interface between the warmer, turbulent epilimnion and the quiescent, colder hypolimnion is called thermocline. This vertical density layering is referred to as density stratification as previously introduced. Apart from density stratification due to a temperature gradient between the epilimnion and hypolimnion (thermal stratification), it can also be due to a concentration gradient of diluted substances (chemical stratification). In this case, the interface is referred to as chemocline. Further information about the nature of stratification in lakes in the context of entrainment can be found in Thorpe (2007) and Csanady (1972).

A lake is exposed to several mechanisms that provoke turbulent entrainment. The most dominant one is wind shearing the water surface. The motion on the surface produces turbulence, which causes the epilimnion to be well-mixed. Wind also produces a secondary motion, large-scale counter-rotating helical vortices, so-called Langmuir Cells (Thorpe, 2007). Furthermore, at nights the surface of the epilimnion cools down and becomes colder than the near subsurface. Due to the density difference, the colder fluid penetrates downwards producing turbulence. This process is referred to as night time convection. As lakes are not fully isolated ecological systems, inflow can produce turbulence as well. A well-known case is the inflow of diluted salt as its greater density causes the flow to run and produce turbulence on its way to the bottom where it remains.

Density stratification, which acts as a sink of turbulence, arises due to variations of the amount of dissolved solids, variation in suspended particles and differences in temperature. Differences in temperature lead to thermal stratification being the most dominant process. Imboden & Wüest (1995) describe the evolution of thermal stratification by three factors: firstly, lakes are stagnant. In such stagnant systems molecular diffusion is

dominant which allows for stable temperature gradients between the epilimnion and hypolimnion. Secondly, water in lakes has long residence times. Since processes like heating, cooling as well as chemical processes develop rather slowly, the flow within the lake, as well as water exchange rates must not be too fast to allow for stratification. Thirdly, as lakes are sometimes very deep, interactions between the surface and the bottom region are rare since the transport of kinetic energy has to overcome long distances.

Hence, stratification in lakes becomes increasingly important the more stagnant, calmer (in terms of residence times) and deeper they are. Mining lakes and water reservoirs are candidates for stable thermal stratification, as they are both considered deep and stagnant.

A stable density interface may suppress the transport e.g. of dissolved oxygen to the hypolimnion. In the epilimnion oxygen is produced by water plants as a result of photosynthesis. Since solar radiation rarely penetrates to the hypolimnion, the supply of dissolved oxygen towards the hypolimnion depends on vertical mixing processes. If vertical mixing is suppressed due to a stable thermocline dissolved oxygen in the hypolimnion can be depleted. It is known that the depletion of dissolved oxygen, known as hypoxia, can lead to poor water quality and mass extinction of living organisms. It is therefore important to understand mixing and stratification in the lake, and if necessary intervene to avoid deterioration.

3 Fundamentals of entrainment and case description

This section provides a definition of turbulent entrainment, how turbulent entrainment can be modelled and outlines the simulations that have been performed.

Fehler! Verweisquelle konnte nicht gefunden werden. demonstrates the evolution of mixing in a two-layer density stratified fluid over a domain of 15m x 5m x 8m. The two subfigures show two temporal states of a representative section of a lake. In both subfigures the temperature gradient varies from cold (white shading) in the hypolimnion to warm (dark shading) in the epilimnion. The total temperature difference is 0.15 K. The wind velocity U=1.5 m s^{-1} remains constant over time and acts over the entire surface region at z=0 m. The top subfigure shows the temperature distribution at t_0 when wind starts acting on the surface. The jump in the temperature profile reveals that the cold and warm layers are separated by a thermocline. As soon as wind acts on the surface, turbulence is generated and transported towards the thermocline. This transport is done by turbulent diffusion. The bottom subfigure shows that the epilimnion has become turbulent over time. Turbulent billows “break through” the interface which leads to turbulent entrainment.

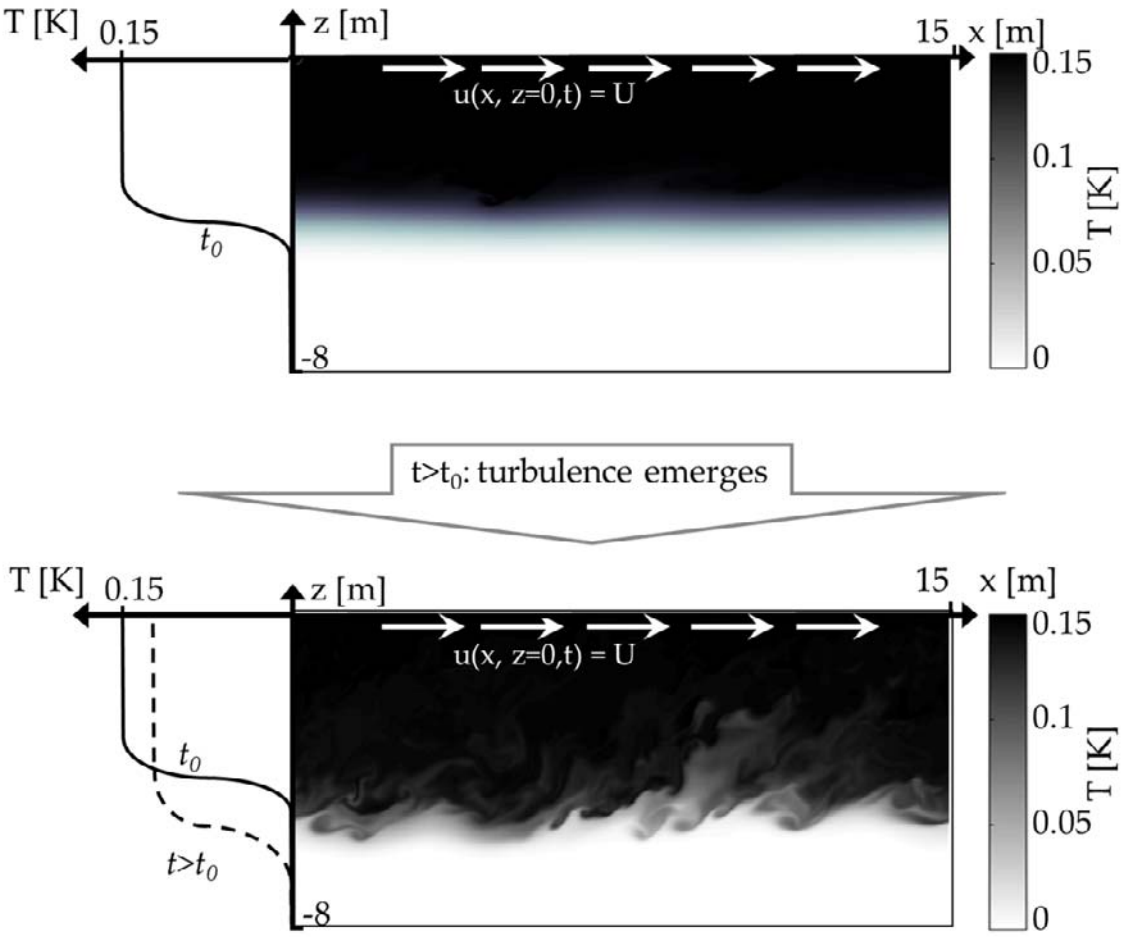

Fig. 1: Sketch of the mechanism of entrainment. t [s] denotes time, T [K] the temperature and U [m s^{-1}] a constant wind velocity imposed at the surface. Homogenisation of the temperature field and shifting of the interface between a turbulent upper and quiescent lower layer takes place as a function of time.

This turbulent entrainment is done e.g. by Kelvin-Helmholtz-instabilities, fine filaments or engulfments of colder water that is mixed into the warmer fluid in the epilimnion by diffusive processes (Carruthers and Hunt, 1986). Consequently, turbulent entrainment changes the temperature profile as the temperature profiles in Figure 1 demonstrate: the epilimnion becomes colder and deeper due to cold fluid from the hypolimnion that is entrained into and mixed in the warmer top layer. At the same time, the interface decends as a function of time. After mixing a weaker density gradient remains as time step $t>t_0$ [s] compared to $t=t_0$ [s] reveals.

The change of the interface height over time is expressed as the entrainment velocity w_e [m s^{-1}] (Fernando, 1991)

$$w_e = dh/dt \tag{1}$$

with h [m] the interface height measured from the surface. The temporal change of the interface height is difficult to determine in field and laboratory experiments and in numerical simulations. This difficulty rises from changes of the interface that can be either reversible or irreversible. Reversible changes are e.g. internal waves that move the interface around its initial position and do not contribute to mixing across the interface. Irreversible changes are due to entrainment and are the only contributions that change the interface height. Although the incorporation of reversible changes in field and laboratory experiments and numerical simulations is usually not desired, they are detected as well. It is therefore desirable to determine the entrainment velocity, w_e, incorporating only irreversible changes using a non-dimensional entrainment rate E [-] and a characteristic velocity scale, u_c [m s^{-1}], in order to model *equation (1)*. It is

$$w_e = E\, u_c \tag{2}$$

The benefit that arises from the introduction of a non-dimensional entrainment rate is that it can be employed in various similar applications without the determination of the temporal change of the interface height.

In the present investigation the shear velocity, u_τ [m s^{-1}], is used as a characteristic velocity since it is directly related to the shear imposed at the surface. According to Fernando (1991) the entrainment rate relates to the Richardson number

$$E \sim Ri^{-1} \qquad Ri = \beta\, g\, h\, \Delta\theta / u_\tau^2 \tag{3}$$

with β [K^{-1}] the thermal expansion coefficient and g [m s^{-2}] the gravitational constant. The Richardson number relates potential energy due to a static temperature difference $\Delta\theta$ [K] to kinetic energy which arises as a result of the friction velocity at the surface. The Richardson number can also be seen as an indicator for the stability of the interface.

The uncertainty about the detection of the interface and the determination of the entrainment rate is due to insufficient possible control of the boundary conditions in field and laboratory experiments at low Reynolds numbers that have been carried out in research so far. Therefore, numerical simulations should not only model turbulence but also provide the required control of the boundary conditions. Direct Numerical Simulations (DNS) can provide these requirements as it numerically solves the Navier-Stokes-Equation in the whole range of spatial and temporal scales. It is thus able to resolve turbulent entrainment as it provides e.g. velocities, temperatures and heat fluxes over the entire domain. The DNS code SPARKLE (van Reeuwijk *et al.,* 2008 and Craske & van Reeuwijk, 2015), that has been applied in this work, provides the required data to investigate the position of the interface and the determination of the entrainment rate.

In the course of the investigation eight different simulations have been carried out on a grid of (L_x x L_y x L_z) = (15m x 5m x 8m) at a resolution of 768 x 256 x 640 over 7200s. The simulations differed in the initial temperature difference, $\Delta\theta_{init}$ [K], between the layers as to provide eight different Richardson numbers (table 1), hence eight interfaces of varying stability. Runs 1 to 7 comprise a gradually increasing temperature differences between the two layers and hence a gradually increasing stability of the interface. Run 8 is chosen to be of very large Richardson number to ensure the interface remains stable throughout the simulation time. This run, therefore, provides an upper limit to the relevant range of Richardson numbers.

Table 1: Temperature differences and Richardson numbers characterising the considered runs

Run	1	2	3	4	5	6	7	8
$\Delta\theta_{init}$ [K]	0.05	0.10	0.15	0.20	0.25	0.30	0.35	2.00
Ri [-]	10	20	30	41	51	60	80	414

4 Background Potential Energy as entrainment indicator

Different methods to determine the entrainment rate are in use as e.g. described in Sullivan *et al.* (1998). The most widely used example in field measurements is to interpret the interface height as the distance from the lake surface to the inflection point of the temperature profile. Despite its common use, it measures reversible changes of the interface height (e.g. internal waves), which results in uncertainty. Thus, a different method that only considers irreversible change of the interface height based on the background potential energy has been developed and evaluated. This method and its capability to predict the entrainment rate are briefly described in this section. A more detailed description can be found in Beyer (2014).

BPE is the minimum potential energy determined upon rearranging the density field (Lorenz, 1955) as ***Fehler! Verweisquelle konnte nicht gefunden werden.*** illustrates. The left subfigure outlines the density field before rearranging where each cell of the x-z-domain is of a specific density. It can easily be seen that the cells arrange in an internal wave-like structure. The right figure outlines the density field after rearranging. The BPE of the field can now easily be gotten in DNS from

$$E_B = \int_0^{L_z} \rho_B \, g \, L_x \, L_y \, z \, \mathrm{d}z \tag{4}$$

where E_B [J] is the BPE calculated by the DNS code SPARKLE and ρ_B [kg m^{-3}] the background potential density of the rearranged field. After using the identity of ρ_B, rearranging and integrating (see appendix) an expression for the interface height yields (Beyer, 2014)

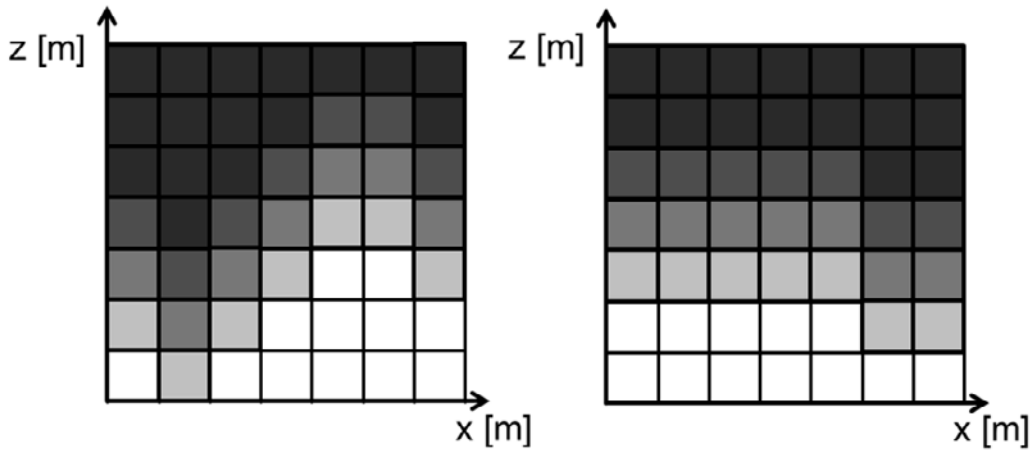

Fig. 2: Visualisation of the BPE in a numerical grid. The left subfigure visualises the distribution of potential energy before rearranging, the right subfigure upon rearranging. Light shading represents lower potential energy levels (lower temperatures).

$$h_{BPE} = \sqrt{L_z^2 + \frac{2E_B}{\beta\, g\, \Delta\theta\, L_x L_y}} \tag{5}$$

As opposed to common methods, *equation (5)* does not incorporate reversible changes of the interface. Indeed, only irreversible mixing due to diffusion is considered. Since turbulence is transported continuously to the interface one would expect the interface height to change in a continuous manner as well. This trend is shown in **Fehler! Verweisquelle konnte nicht gefunden werden.**, which plots the entrainment rate against the Richardson number. Two different entrainment assumptions are provided: An inverse of the Richardson number, which is commonly applied as a proportional entrainment law and an exponential power law fit to the DNS data. Both suggest that the higher the Richardson number, i.e. the more stable the interface is, the lower the entrainment rate. Although the sample size is very small, the fit of the data is remarkably good. The low Root-mean-square deviation (RMSD) of $0.9 \cdot 10^{-3}$ and the very large adjusted R^2-value of 0.98 highlight that the BPE method is almost free of noise.

However, the friction velocity u_τ was found to change significantly over time. This imposes an important limitation to the interpretation of the data since the friction velocity changes so rapidly in time that the Richardson number might not be representative for the turbulence at the density interface. Therefore, it is questionable whether the Richardson number in its present form is a suitable entrainment parameter. Indeed, a definition that is based upon the turbulence near the interface might be more appropriate.

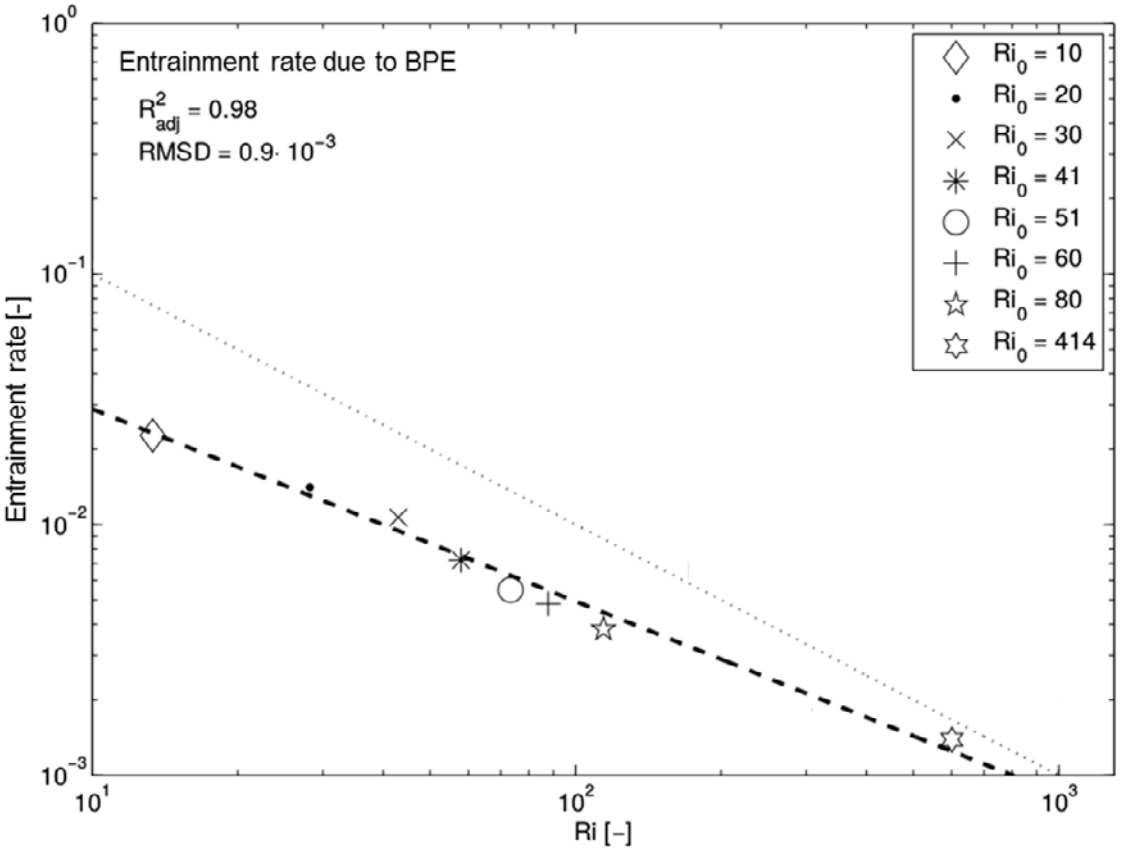

Fig. 3: Entrainment rate of the BPE against the Richardson Number Ri. The dashed line is an exponential power law fit, $E=2.81\ Ri^{-1.31}$, of the simulation results. The simulation results are denoted by markers. The dotted line refers to $E=Ri^{-1}$.

5 Conclusion

This report has addressed turbulent entrainment in lakes. The ecological quality of lakes partly depends upon entrainment and stratification. Although in limnology it is important to understand the nature of entrainment and stratification, both processes are not fully understood. This report has outlined the main entrainment and stratification characteristics in lakes. It has presented a new technique to determine the entrainment rate based upon background potential energy. The results confirm the dependence of the entrainment rate on the Richardson number and are almost free of statistical noise interpreted by the adjusted R^2 and the RMSD. However, the temporal dependence of the friction velocity, interpreted as characteristic velocity, indicates that the Richardson number in its present form is not representative for the turbulence near the interface. Therefore, more research needs to be carried out regarding an adequate characteristic velocity.

6 Appendix

The appendix addresses the derivation of the interface height using BPE. The BPE is defined in *equation* (*4)* as

$$E_B = \int_0^{L_z} \rho_B \; g \; L_x \; L_y \; z \;\; \mathrm{d}z \tag{4}$$

with

$$\rho_B = \rho_0(1 - \beta\theta_B) \tag{A.1}$$

the background potential density of the rearranged domain where ρ_0 [kg m^{-3}] is the density of the quiescent layer, β [K^{-1}] the thermal expansion coefficient and θ_B [K] is the temperature of that layer. The BPE is evaluated from the DNS data at every time step. To translate the BPE to an interface height *h* [m], the domain size L_z [m] can be split into a mixed layer *h* and the quiescent layer $L_z - h$. In this case, *equation (4*) can be evaluated analytically with result

$$E_B = \int_0^{L_z} \; g \; \rho_0(1 - \beta\theta_B) \;\; L_x \; L_y \;\; z \;\; \mathrm{d}z$$

$$\Leftrightarrow E_B = -\int_h^{L_z} \; g \; \beta\Delta\theta_B \;\; L_x \; L_y \;\; z \; \mathrm{d}z = 0.5 \; g \; \beta \; \Delta\theta_B \;\; L_x \; L_y \; (h^2 - L_z^2) \tag{A.2}$$

In the second line, it was assumed that the BPE is zero in the quiescent bottom layer and that $\theta_B = \Delta\theta_B$ in the turbulent top layer. Upon rearranging, it follows that the interface height, *h*, is as stated in *equation (5)*.

7 Literature

Beyer, M. (2014). *Direct numerical simulation of mixing in stratified fluids.* Institute of Hydraulic Engineering and Water Resources Management RWTH Aachen University: MSc Thesis.

Carruthers, D., & Hunt, J. (1986). *Velocity fluctuations near an interface between a turbulent region and a stable layer.* J. Fluid. Mech.165:475-501.

Craske, J., & van Reeuwijk, M. (2015). *Energy dispersion in turbulent jets. Part 1. Direct simulation of steady and unsteady jets.* J. Fluid Mech. 763: 500-37.

Csanady, G. (1972). *Frictional currents in the mixed layer at the sea surface.* J. Phys. Oceanogr. 2:498-508.

Fernando, H. (1991). *Turbulent mixing in stratified fluids.* Ann. Rev. Fluid Mech. 23:377-95.

Imboden, D., & Wüest, A. (1995). *Mixing mechanisms in lakes: Physics and chemistry in lakes.* Springer Verlag.

Jonker, H., van Reeuwijk, M., Sullivan, P., & Patton, E. (2013). *On the scaling of shear-driven entrainment: a DNS study.* J. Fluid Mech. 732: 150-65.

Lorenz, E. (1955). *Available potential energy and the maintenance of the general circulation.* Tellus 7:157-67.

Sokolofsky, A., & Jirka, G. (2004). *Mixing in lakes and reservoirs.* Retrieved 10 20, 2015, from Texas A&M University. Coastal & Ocean Engineering Division: https://ceprofs.civil.tamu.edu/ssocolofsky/ocenx89/downloads/book/socolofsky_jirka.pdf

Sullivan, P., Moeng, C., Stevens, B., Lenschow, D., & Mayor, S. (1998). *Structure of the entrainment zone capping the convective atmospheric boundary layer.* J. Atmos. Sc. 55: 3042-64.

Thorpe, S. (2007). *An introduction to ocean turbulence.* Cambridge: Cambridge University Press.

van Reeuwijk, M., Jonker, H., & Hanjalić, K. (2008). *Wind and boundary layers in Rayleigh-Bénard convection. I. Analysis and modeling.* Physical Review E 77.3.

Authors' addresses

Magnus Beyer and Maarten van Reeuwijk
Department of Civil and Environmental Engineering
Imperial College London
London SW7 2BU
United Kingdom

Holger Schüttrumpf
RWTH Aachen University
Lehrstuhl für Wasserbau und Wasserwirtschaft
Mies-van-der-Rohe Straße 17
52056 Aachen
Germany